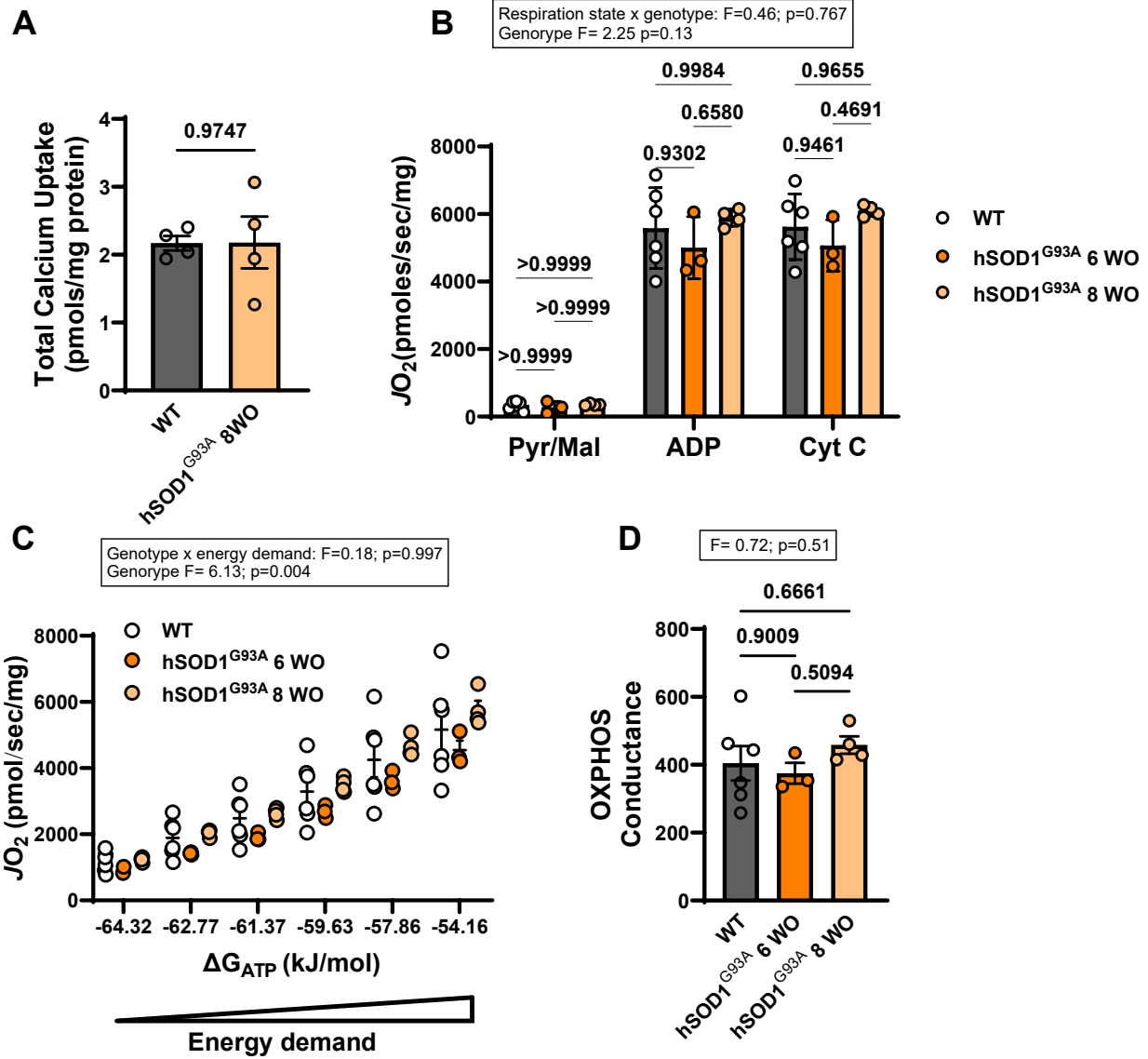
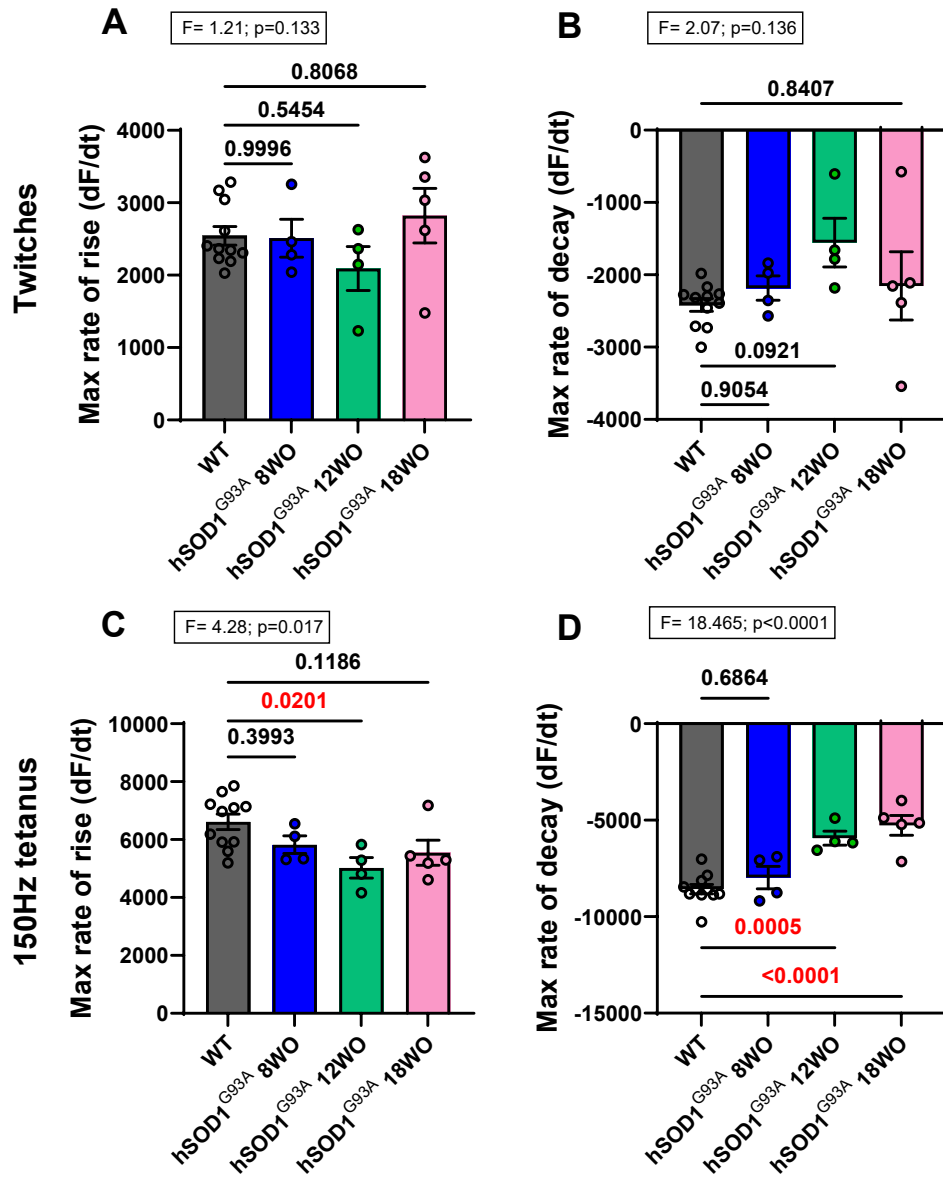


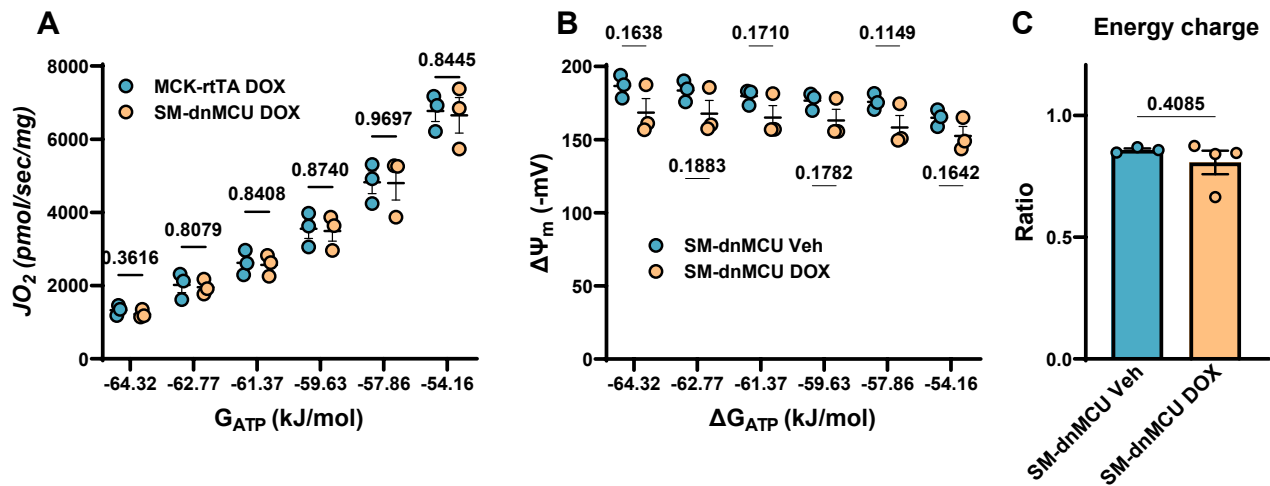
Supplementary materials



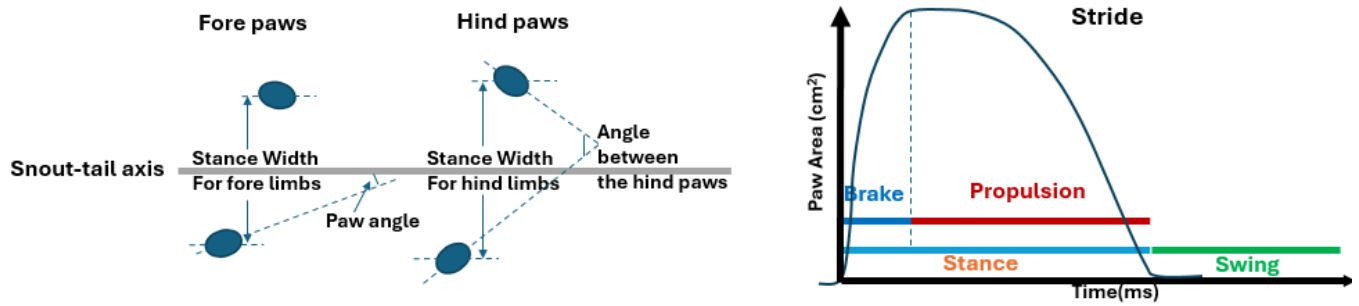
Supplementary Figure 1: Lack of mitochondrial bioenergetic defect in hindlimb muscle mitochondria isolated from 6-8 week-old in hSOD1^{G93A} mice. (A) Averaged (\pm SEM) mitochondrial Ca²⁺ retention capacity of skeletal mitochondria isolated from 8 weeks old WT and hSOD1^{G93A} mice. **(B)** Averaged (\pm SEM) maximal oxygen consumption (JO_2) at state 2 (Pyr/Mal only) and state 3 (ADP) respiration and with exogenous Cytochrome C (Cyt C) in mitochondria from 6- and 8-week-old hSOD1^{G93A} mice. **(C)-(D)** Averaged (\pm SEM) JO_2 at different energy demand (ADP/ATP ratio) titrated using CK clamp, and OXPHOS conductance **(D)** calculated using the slope of the increase in JO_2 against energy demand (ΔG_{ATP}) in **C**. **A**, Student's *t*-test; **B** and **C**, 2-way ANOVA with repeated measures; and **D**, one-way ANOVA, Tukey *post-hoc* tests. Mouse number, N, for each group were indicated in each graph as individual data points. P values for each comparison were indicated in the graph.



Supplementary Figure 2: Slowed muscle contractile kinetics in hSOD1^{G93A} EDL muscle at more advanced disease stage. (A)-(B) Averaged (\pm SEM) maximal rate of rise in the force development (A) and maximal rate of force decay (B) during the relaxation phase following a twitch stimulation in WT and hSOD1^{G93A} EDL muscles at 8 weeks old (experimental disease onset), 12 weeks old (clinical onset) and 18 weeks old (advanced stage). (C)-(D) Same as A-B, except for following a 500 ms tetanic stimulation at 150 Hz. One-way ANOVA with Tukey *post-hoc* tests; N for each group were indicated in each graph as individual data points. P values for each comparison were indicated in the graph, with statistically significant comparisons highlighted in red.



Supplementary Figure 3. Minimal change in mitochondrial bioenergetic function in SM-dnMCU mice following veh/DOX administration. (A) Averaged (\pm SEM) oxygen consumption and mitochondrial membrane potential **(B)** at different energy demand (ADP/ATP ratio) titrated using CK clamp in mitochondria isolated from hindlimb muscles of 14 weeks old SM-dnMCU mice. **(C)** Averaged (\pm SEM) energy charge in TA muscles at rest calculated from the concentrations of AMP, ADP and ATP measured by LC-MS using $[ATP]+1/2[ADP]/([AMP]+[ADP]+[ATP])$ in 18 weeks old Veh/DOX-treated SM-dnMCU mice. *Student's-t* test or multiple *Student's-t* tests. N for each group were indicated in each graph as individual data points. P values for each comparison were indicated in the graph, with statistically significant comparisons highlighted in red.



Supplementary Figure 4. Schematic for DigiGait parameter calculations. Mouse paw placements (Left) and schematic of DigiGait parameters in one stride cycle (Right).

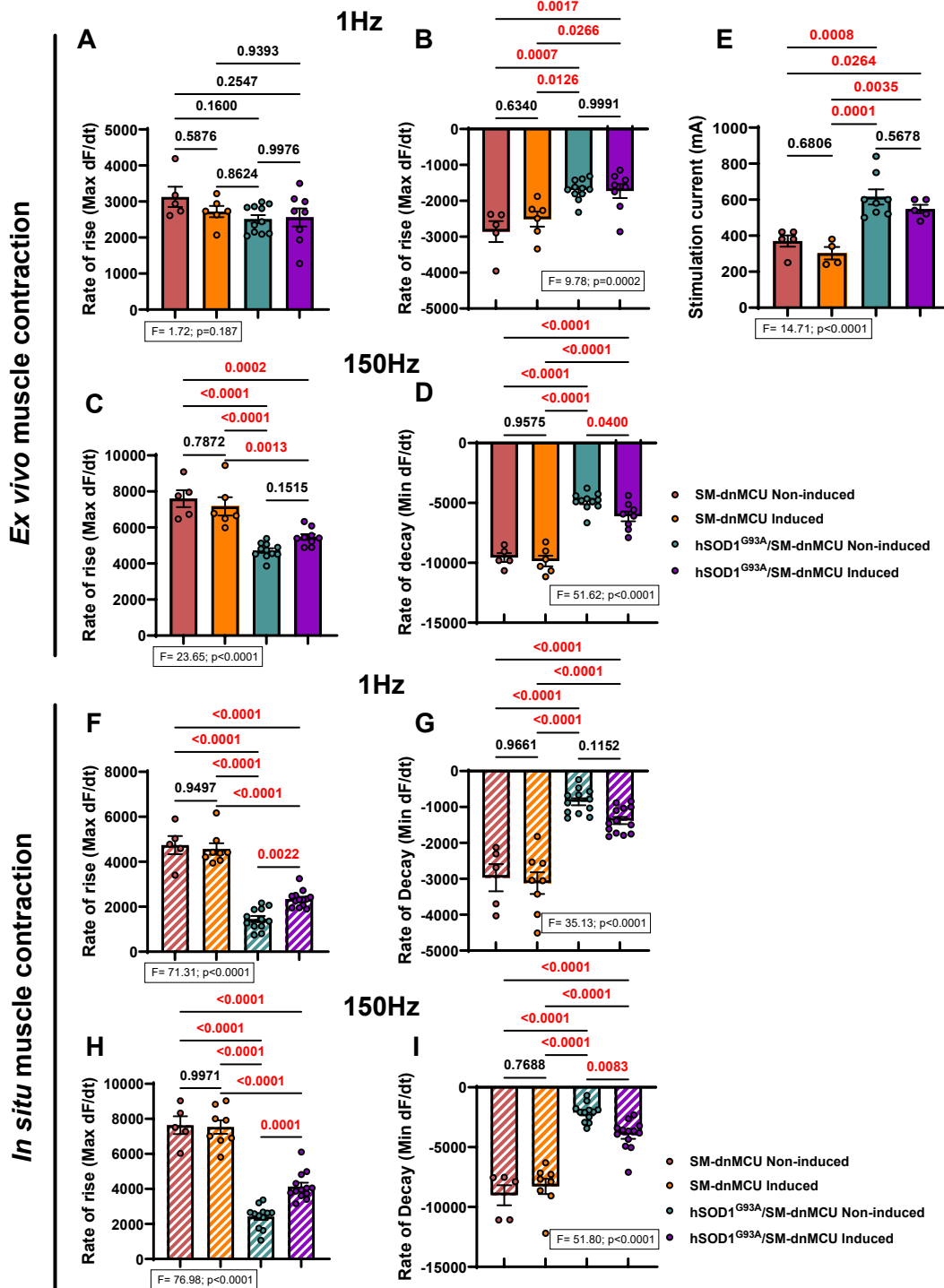
Supplementary Table 1. Description of DigiGait parameters.

Parameter	Unit	Description
Stride duration	s	time duration of one complete stride for one paw
Stance time	s	duration of time the paw is in contact with the belt
Swing time	s	duration of time the paw is not in contact with the belt
Propulsion duration	s	from maximum paw contact to just before the swing phase
Stance width	cm	combined distance from the fore/hind paws to the snout-tail axis
Stride length	cm	average distance between two strides of the same paw
Stride frequency	# of strides/s	number of complete strides per second
Absolute paw angle	degree	angle of the paw in relation to the snout-tail axis of the animal
Step angle variability	degree	standard deviation of the angle between the hind paws as a function of SL and SW

Supplementary Table 2. Summary of statistical analyses for Digigait measurements.

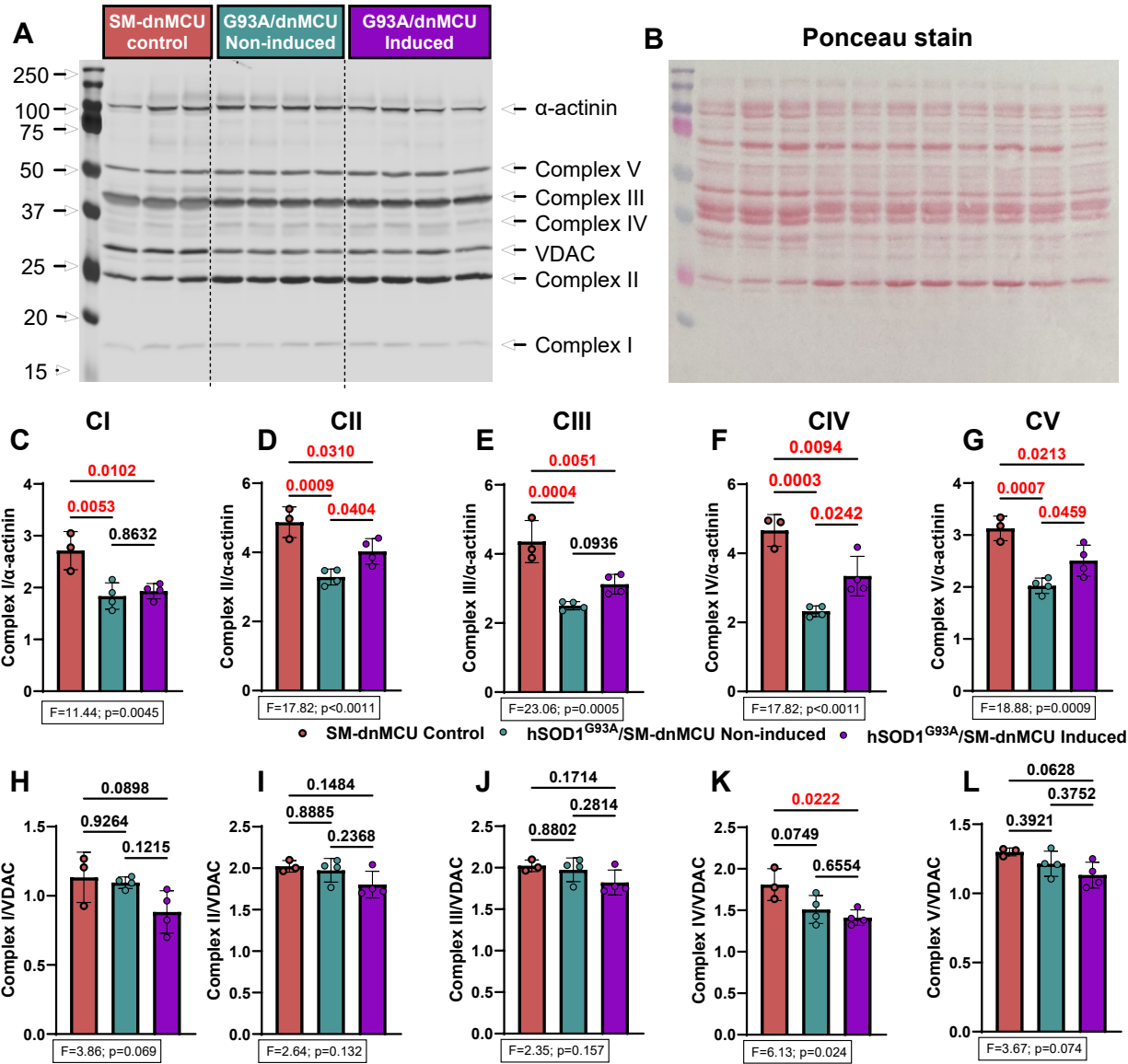
Gait parameters of SM-dnMCU control (n=9) hSOD1-non induced (10), and hSOD1-induced (14) mice hindlimbs during disease progression							
		12 weeks old			14 weeks old		
		SM-dnMCU control (9)	hSOD1/SM-dnMCU, non-induced(11)	hSOD1/SM-dnMCU induced(14)	SM-dnMCU (9)	hSOD1/SM-dnMCU non-induced (10)	hSOD1/SM-dnMCU induced (12)
stride duration(s)	Mean± SEM	0.27±0.0089	0.32±0.0076* #	0.28±0.0033	0.26±0.0102	0.33±0.0071* #	0.29±0.0040*
	Vs. SM-dnMCU control		*p<0.0001	p=0.6868		*p<0.0001	*p=0.0104
	Vs. hSOD1/SM-dnMCU induced		#p<0.0001			#p<0.0001	
stance time	Mean± SEM	0.16±0.0052	0.18±0.0042* #	0.16±0.0044	0.15±0.0093	0.18±0.0054*	0.17±0.0022
	Vs. WT		*p=0.0116	p=0.9842		*p=0.0003	*p=0.0236
	Vs. hSOD1/SM-dnMCU induced		#p=0.0074			P=0.2302	
swing time (s)	Mean± SEM	0.11±0.0070	0.14±0.0070* #	0.11±0.0028	0.10±0.0043	0.14±0.0055* #	0.11±0.0051
	Vs. SM-dnMCU control		*p=0.0004	p=0.6532		*p<0.0001	p=0.5299
	Vs. hSOD1/SM-dnMCU induced		#p=0.0016			#p=0.0002	
propulsion duration (s)	Mean± SEM	0.11±0.0051	0.14±0.0054* #	0.12±0.0033	0.10±0.0087	0.14±0.0054*	0.13±0.0025
	Vs. SM-dnMCU control		*p=0.0017	p=0.4427		*p<0.0001	*p=0.0095
	Vs. hSOD1/SM-dnMCU induced		#p=0.0216			p=0.1134	
stance width (cm)	Mean± SEM	2.45±0.1195	2.36±0.0789	2.45±0.0959	2.53±0.1041	2.02±0.0377* #	2.42±0.0747
	Vs. SM-dnMCU control		P=0.8933	P=0.9723		* p=0.0008	P=0.6381
	Vs. hSOD1/SM-dnMCU induced		p=0.7380			#p=0.0058	
stride length(cm)	Mean± SEM	5.31±0.1713	6.21±0.1275* #	5.60±0.0594	5.3±0.2192	6.27±0.1119* #	5.77±0.0810*
	Vs. SM-dnMCU control		*p=0.0003	P=0.8552		*p<0.0001	*p=0.0100
	Vs. hSOD1/SM-dnMCU induced		#p=0.0004			#p=0.0073	
stride frequency (steps/s)	Mean± SEM	3.72±0.1144	3.15±0.0813* #	3.60±0.0350	3.91±0.1695	3.06±0.0735* #	3.5±0.0492*
	Vs. SM-dnMCU control		*p=0.0007	P=0.9994		*p<0.0001	*p=0.0019
	Vs. ALS-induced		#p=0.0002			#p=0.0006	
Absolute paw angle (degree)	Mean± SEM	22.66±1.5871	18.82±1.5490* #	22.33±1.0497	23.58±0.7987	17.83±0.7225* #	22.63±0.9399
	Vs. SM-dnMCU control		*p=0.0347	P=0.8883		* p=0.0036	P=0.8287
	Vs. hSOD1/SM-dnMCU induced		ns, p=0.0556			#p=0.0100	
step angle variability (degree)	Mean± SEM	10.65±1.3262	14.02±1.5871	11.86±0.9188	9.74±0.9510	18.00±1.6076* #	10.02±0.6993
	Vs. SM-dnMCU control		p=0.0669	P=0.5249		* p<0.0001	P=0.9850
	Vs. hSOD1/SM-dnMCU-induced		P=0.3545			# p<0.0001	

*Significant difference from SM-dnMCU control. # Significant difference from hSOD1^{G93A}/SM-dnMCU induced. Statistically significant comparisons are highlighted in red.

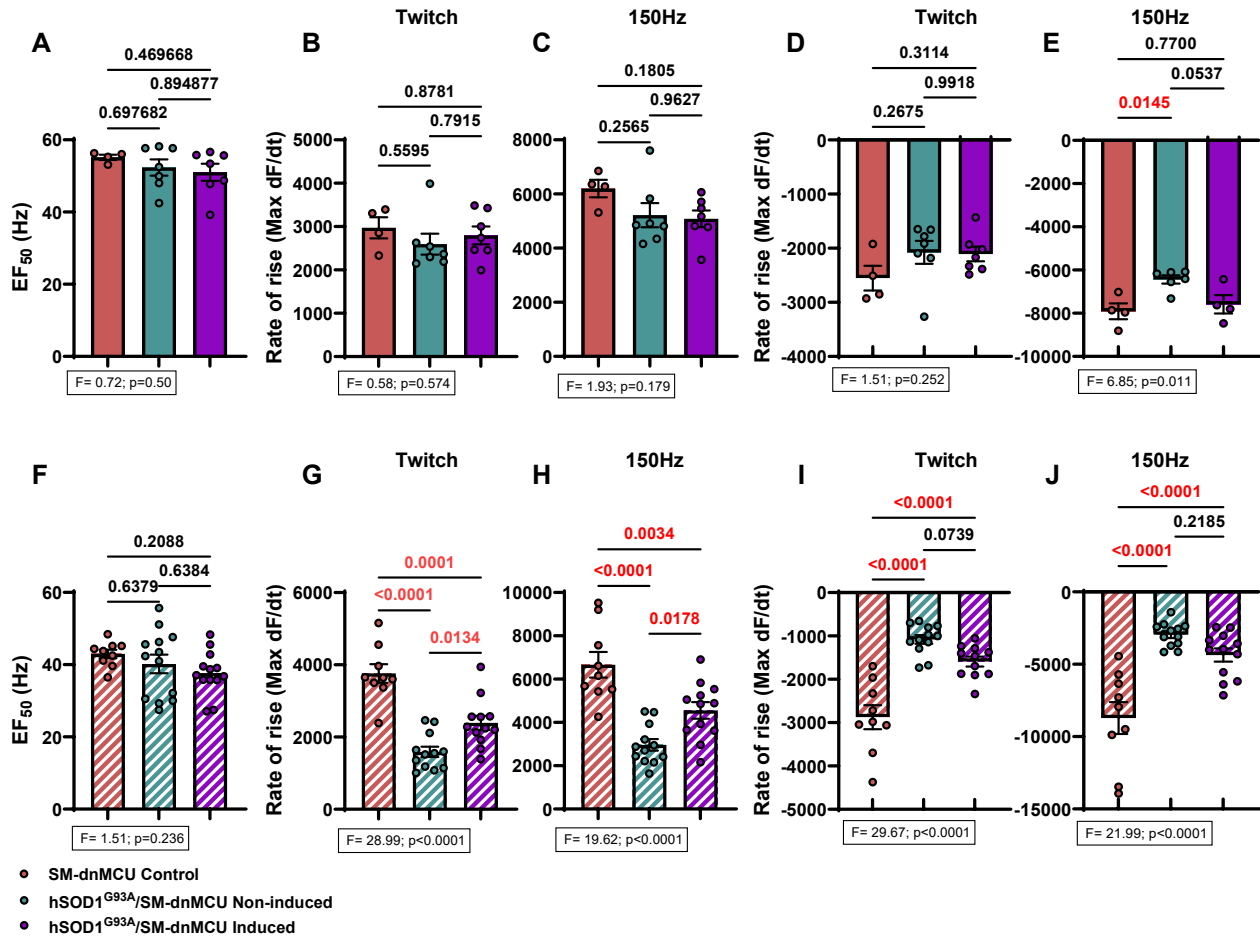


Supplementary figure 5. Kinetics for *ex vivo* and *in situ* muscle contraction in EDL muscles from 18-week-old SM-dnMCU and hSOD1^{G93A}/SM-dnMCU mice with and without dnMCU expression from disease onset. (A)-(B) Averaged (\pm SEM) maximal rate of rise in force development (A) and maximal rate of force decay during the relaxation phase (B) following a twitch stimulation in *ex vivo* muscle contraction. (C)-(D) Same as A-B, except for following a 500 ms tetanic stimulation at 150 Hz.

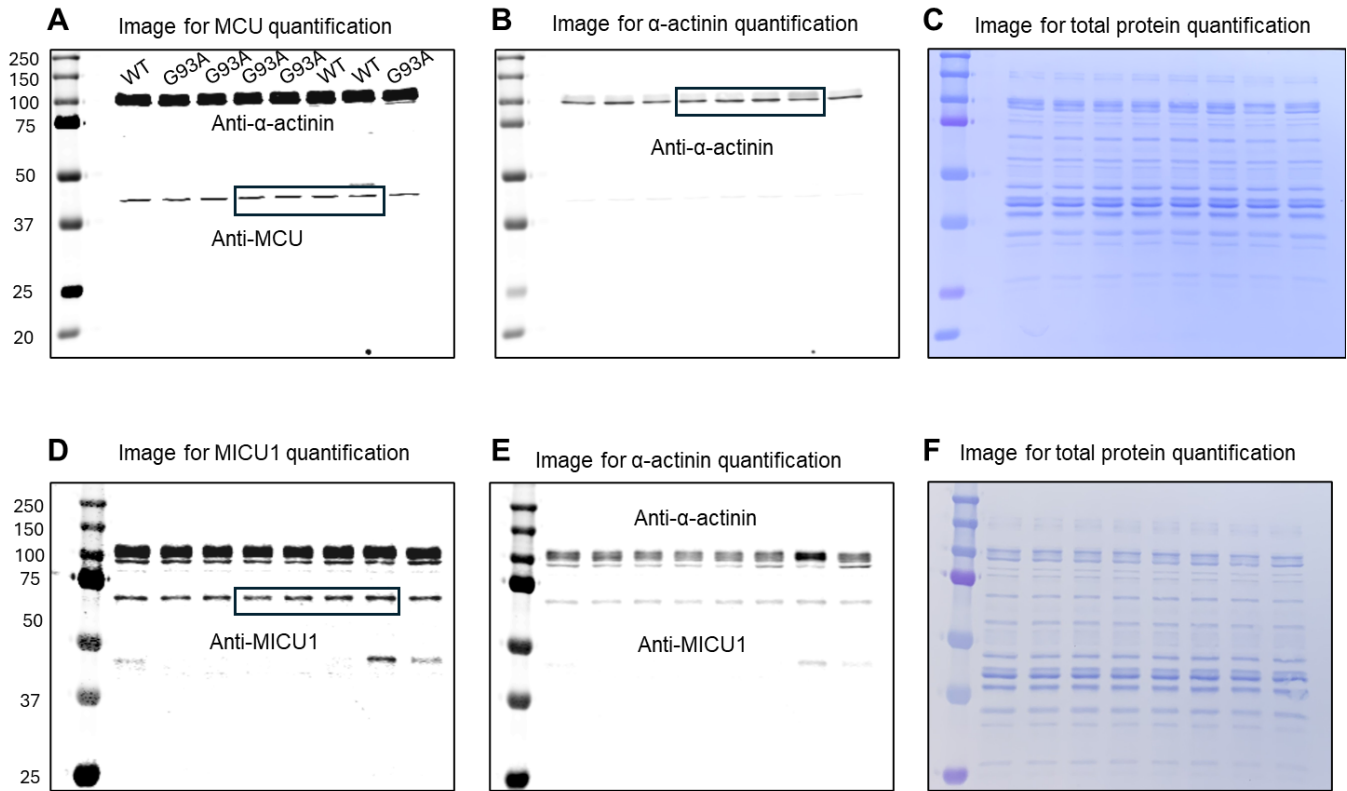
(E) Averaged (\pm SEM) stimulus strength required to elicit maximal contraction in EDL muscles in control and hSOD1^{G93A} compound mice. **(F)-(I)** Same as **A-D**, except for contractions elicited using an *in situ* set up (nerve stimulation). One-way ANOVA with Tukey *post-hoc* tests; N for each group were indicated in each graph as individual data points. P values for each comparison were indicated in the graph, with statistically significant comparisons highlighted in red.



Supplementary Figure 6. Immunoblotting analyses of mitochondrial OXPHOS complexes in TA muscles from DOX-induced or non-induced SM-dnMCU and hSOD1^{G93A}/SM-dnMCU mice from disease onset. (A) Immunoblot image probed for OXPHOS complexes and VDAC. Molecular mass markers are indicated on the left. **(B)** Ponceau stained nitrocellulose membrane to visualize total protein for normalization. **(C)-(G)** Densitometry analysis for Complex I-V normalized to α -actinin. **(H)-(L)** Densitometry analysis for Complex I-V normalized to VDAC. One-way ANOVA with Tukey *post-hoc* tests; N for each group were indicated in each graph as individual data points. P values for each comparison were indicated in the graph, with statistically significant comparisons highlighted in red.



Supplementary Figure 7. Kinetics for *ex vivo* and *in situ* muscle contraction in EDL muscles from 12 weeks old SM-dnMCU and hSOD1^{G93A}/SM-dnMCU mice with dnMCU induction from 4 weeks old. (A) Averaged (\pm SEM) frequencies of stimulation that elicit half of the peak contractile force for each condition. **(B)-(C)** Averaged (\pm SEM) maximal rate of rise in force development following a twitch **(B)** or a 500 ms tetanic stimulation at 150 Hz **(C)** in *ex vivo* muscle contraction. **(D)-(E)** Averaged (\pm SEM) maximal rate of force decay during the relaxation phase following a twitch **(D)** or a 500 ms tetanic stimulation at 150 Hz **(E)** in *ex vivo* muscle contraction. **(F)-(J)** Same as **A-E**, except for contractions elicited using an *in situ* set up (nerve stimulation). One-way ANOVA with Tukey *post-hoc* tests; N for each group were indicated in each graph as individual data points. P values for each comparison were indicated in the graph, with statistically significant comparisons highlighted in red.



Supplementary Figure 8. Full western blot images for MCU and MICU1 in TA muscles at 6 weeks old. (A)-(C). Images for densitometry quantification for MCU in Figure 1 (A), loading control α -actinin (B, acquired at lower gain to avoid signal saturation), and total protein stained with Coomassie blue (C). (D)-(F), same as A-C but for densitometry quantification for MICU1. Rectangle boxes in images were the image cutouts shown in Figure 1C. Molecular mass markers are indicated on the left for each set of images.

Supplementary Table 3, Primary and secondary antibodies used in the study.

	Manufacturer	Application	Dilution	Catalog #
Anti- α -actinin	Sigma-Aldrich	Western Blot	1:2000	A7732
Anti-MCU	Invitrogen	Western Blot	1:2000	PA5-68153
Anti-MICU1	Invitrogen	Western Blot	1:2000	PA5-83371
Mitochondrial OXPHOS complex	Abcam	Western Blot	1:10000	ab110413
Anti-VDAC1/Porin+VDAC3	Abcam	Western Blot	1:2000	Ab14734
SV2 (Synaptic vesicle protein 2)	Developmental Studies Hybridoma Bank	Immunofluorescence (Primary)	1:100	AB_2315387
Znp-1 (Synaptotagmin 2)	Developmental Studies Hybridoma Bank	Immunofluorescence (Primary)	1:150	AB_2315626
2H3 (Neurofilament)	Developmental Studies Hybridoma Bank	Immunofluorescence (Primary)	1:150	AB_531793
Alexa Fluor 488-conjugated α -Bungarotoxin	Invitrogen	Immunofluorescence (Secondary)	1:1000	B13422
Alexa Fluor 594 Goat anti Mouse	Invitrogen	Immunofluorescence (Secondary)	1:500	PIA32742
IRDye® 800CW Goat anti-Rabbit IgG	Li-COR Biotech	Western Blot (Secondary)	1:10000	NC9816235
IRDye® 800CW Goat anti-mouse IgG	Li-COR Biotech	Western Blot (Secondary)	1:10000	NC9401841